J Low Temp Phys
https://doi.org/10.1007/s10909-018-1906-3

# Hafnium Films and Magnetic Shielding for TIME, A mm-Wavelength Spectrometer Array

**J. Hunacek[1] · J. Bock[1,2] · C. M. Bradford[1,2] · V. Butler[6] · T.-C. Chang[2] · Y.-T. Cheng[1] · A. Cooray[4] · A. Crites[1] · C. Frez[2] · S. Hailey-Dunsheath[1] · B. Hoscheit[1] · D. W. Kim[5] · C.-T. Li[3] · D. Marrone[5] · L. Moncelsi[1] · E. Shirokoff[7] · B. Steinbach[1] · G. Sun[1] · I. Trumper[5] · A. Turner[2] · B. Uzgil[8] · A. Weber[2] · M. Zemcov[7]**

Received: 30 October 2017 / Accepted: 29 March 2018
© Springer Science+Business Media, LLC, part of Springer Nature 2018

**Abstract** TIME is a mm-wavelength grating spectrometer array that will map fluctuations of the 157.7-mm emission line of singly ionized carbon ([CII]) during the epoch of reionization (redshift $z \sim 5$–9). Sixty transition-edge sensor (TES) bolometers populate the output arc of each of the 32 spectrometers, for a total of 1920 detectors. Each bolometer consists of gold absorber on a $\sim 3 \times 3$ mm silicon nitride micro-mesh suspended near the corners by $1 \times 1 \times 500$ μm silicon nitride legs targeting a photon-noise-dominated NEP $\sim 1 \times 10^{-17}$ W/$\sqrt{\text{Hz}}$. Hafnium films are explored as a lower-$T_c$ alternative to Ti (500 mK) for TIME TESs, allowing thicker support legs for improved yield. Hf $T_c$ is shown to vary between 250 and 450 mK when varying the resident Ar pressure during deposition. Magnetic shielding designs and simulations are presented for the TIME first-stage SQUIDs. Total axial field suppression is predicted to be $5 \times 10^7$.

**Keywords** Spectrometers · Bolometers · Transition-edge sensors · Hafnium · Magnetic shielding

✉ J. Hunacek
jhunacek@caltech.edu

1 California Institute of Technology, Pasadena, USA

2 Jet Propulsion Laboratory, Pasadena, USA

3 Academia Sinica Institute of Astronomy and Astrophysics, Taipei, Taiwan

4 University of California Irvine, Irvine, USA

5 University of Arizona, Tucson, USA

6 Rochester Institute of Technology, Rochester, USA

7 University of Chicago, Chicago, USA

8 Max Planck Institute for Astronomy, Heidelberg, Germany

Published online: 06 April 2018

## 1 Introduction

TIME [1–3] is a mm-wavelength spectrometer array [4] that will map fluctuations of the 157.7-μm emission line of singly ionized carbon ([CII]) during the epoch of

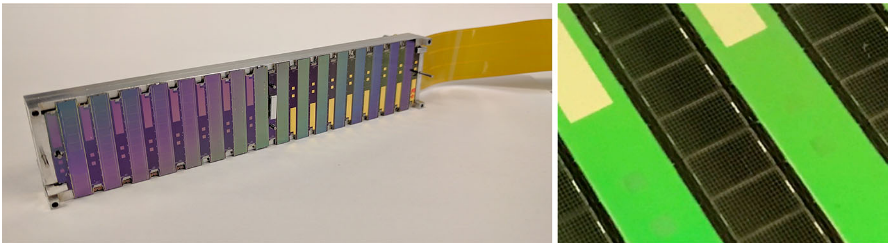

**Fig. 1** Left A prototype TIME high-frequency detector module, responsible for 12 spectral channels for each of 16 spectrometers. Right Fully released silicon nitride micro-mesh absorbers in a prototype TIME high-frequency detector sub-module (Color figure online)

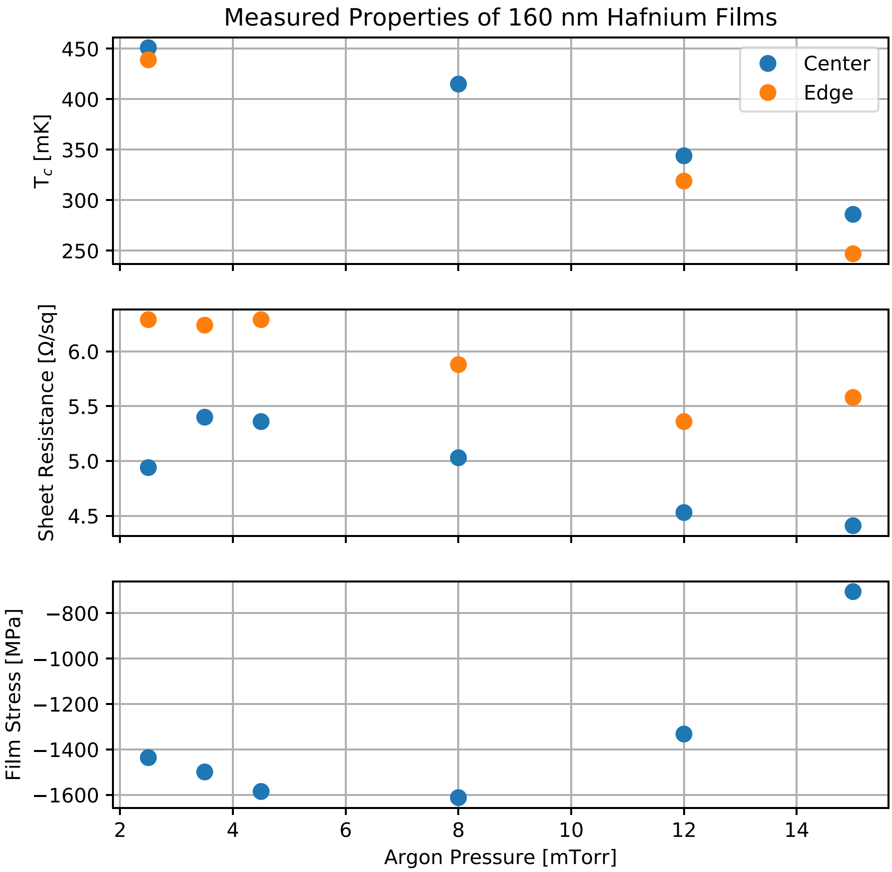


**Fig. 2** Measured properties of Hf films produced at the JPL Microdevices Laboratory (MDL)(Color figure online)

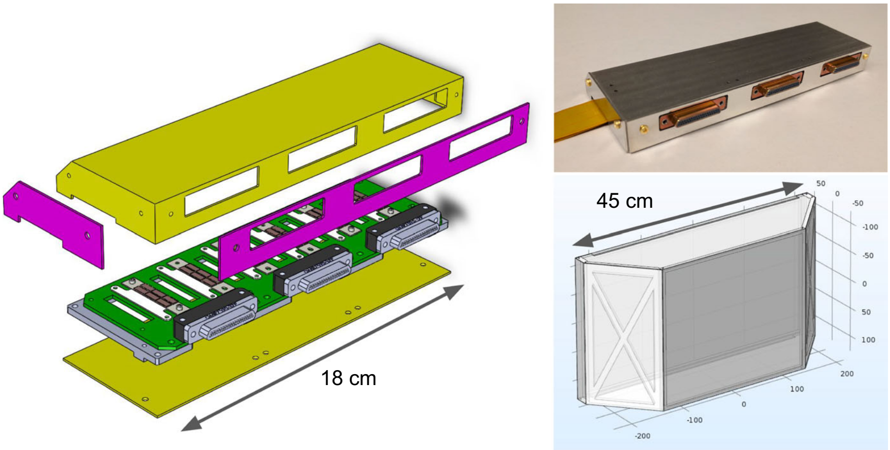


**Fig. 3** Left An exploded render of a TIME SQUID daughtercard housing. Superconducting material (Al) is shown in yellow, and high-$\mu$ metal (A4K) is shown in magenta. Top right One of the 12 TIME SQUID daughtercards. Bottom right The high-$\mu$ box that surrounds the 12 TIME SQUID daughtercards (Color figure online)

reionization (redshift $z \sim 5$–9) [5,6]. A $14 \times 0.43$ arcmin instantaneous field of view corresponding to $16 \times 1$ spatial pixels is sampled by two banks of single-polarization grating spectrometers (32 spectrometers in total). Each spectrometer consists of an input feedhorn, a parallel-plate waveguide, and a curved diffraction grating (similar to that used in Z-Spec [7,8]) with resolving power $R = 170$ and spectral range 183–326 GHz. The output arc of each spectrometer is sampled at $R \sim 100$ with 60 TES bolometers, of which 16 on the band edges are used for atmospheric monitoring and removal. The TESs (1920 in total) are designed in close-packed buttable arrays of 8 spatial $\times$ 12 spectral (high frequency) or 8 spatial $\times$ 8 spectral (low frequency) pixels and will be operated from a 250 mK base temperature with a photon-noise-dominated NEP $\sim 1 \times 10^{-17}$ W/$\sqrt{\text{Hz}}$. Each bolometer consists of gold absorber on a $2.3 \times 3$ mm (high frequency) or $3.5 \times 3$ mm (low frequency) silicon nitride micro-mesh suspended near the corners by $1 \times 1 \times 500$ µm silicon nitride legs. Absorbed radiation is thermally coupled to elemental Al and Ti TESs connected in series. (Al is used in higher-loading laboratory conditions.) Detector readout uses SQUIDs and time-domain multiplexing. Prototype TIME high-frequency detector arrays with fully released micro-meshes are shown in Fig. 1.

## 2 Hafnium Films

Current TIME detectors use a Ti TES with $T_c = 495$ mK. Because we operate at a base temperature of 250 mK, reducing to $T_c \sim 350$ mK would allow us to use 4$\times$ thicker suspension legs for the micro-mesh absorbers at the same saturation power without phonon noise penalties, thus improving device yield and durability. Toward that end, 160-nm Hf films were deposited on silicon nitride-coated silicon wafers at the JPL Microdevices Laboratory (MDL). Resident argon pressure in the deposition chamber was controlled between 2.5 and 15 mTorr during the sputtering process for different

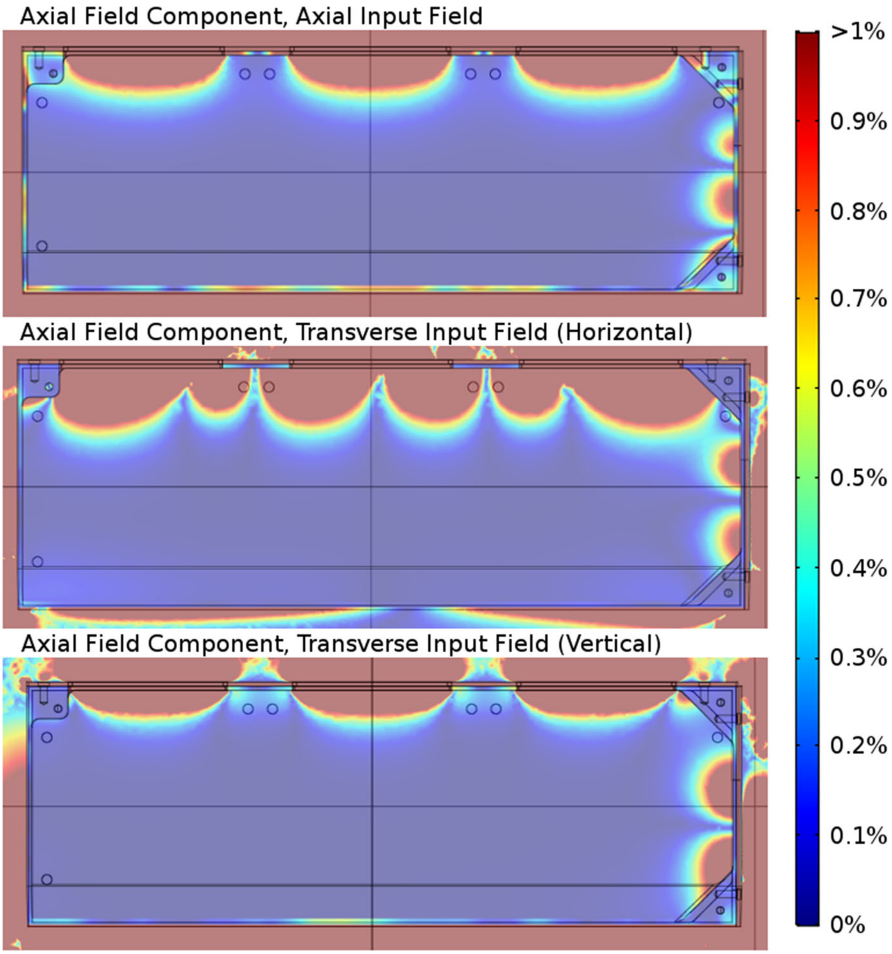


**Fig. 4** COMSOL simulations of the magnetic field suppression of the first-stage SQUID daughtercard enclosure (superconducting box with high-$\mu$ connector plates). The axial component of the magnetic field in the plane of the SQUIDs is shown. The three connector holes are located at the top in this view, and the entrance for the superconducting flex-circuit is on the right (Color figure online)

samples to influence the stress of the resulting films. Results are shown in Fig. 2. Films had a room temperature resistivity of approximately 5.5 $\Omega/\Box$. $T_c$ was found to vary between 250 and 450 mK with good center-to-edge uniformity, indicating that the desired 350 mK is achievable with Hf. TIME-style devices with Hf TESs are being processed and will be tested in the near future.

## 3 Magnetic Shielding

### 3.1 First-Stage SQUID Module Enclosures

The first-stage SQUIDs in TIME are located on 12 PCB daughtercards at the 250 mK stage, each of which is responsible for either 192 or 128 TES bolometers (32 rows

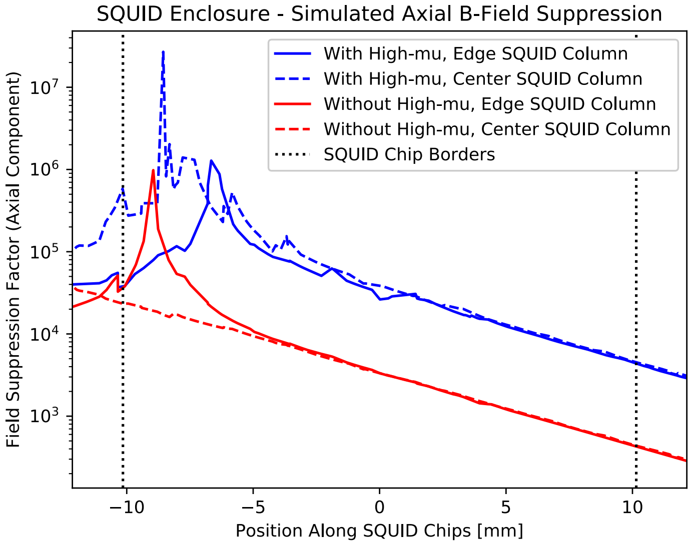


**Fig. 5** COMSOL simulations of the magnetic field suppression of the first-stage SQUID daughtercard enclosure along the SQUID chips. Addition of high-$\mu$ connector plates (shown in magenta in Fig. 3) increases field suppression by a factor of 10 (Color figure online)

$\times$ 6 columns for high-frequency modules; 32 rows $\times$ 4 columns for low frequency). Three 37-pin micro-D connectors mate to the signal distribution motherboard, and a set of superconducting flex-circuits (one per multiplexing column) carries traces to the detectors. Each daughtercard is enclosed in a superconducting box (Fig. 3) to reduce sensitivity to AC magnetic fields. Additional 1-mm-thick high-$\mu$ plates (shown in magenta) are mounted on the faces containing holes for the connectors and flex-circuits; these are intended to direct magnetic field lines around the holes and reduce field ingress.

The daughtercard enclosure was simulated with COMSOL 5.2a. The high-mu material used $\mu_r = 52,000$, which is representative of Amuneal A4K at low temperatures [9]. Superconducting material used $\mu_r = 10^{-5}$, and magnetic insulation was applied to all superconducting surfaces. The final mesh contained 3.7 million elements. Figure 4 shows the component of the magnetic field normal to SQUIDs in the SQUID plane for incident magnetic fields along three axes. Note that the shielding can rotate transverse input fields, producing an axial field component near holes in the enclosure. Figure 5 plots the component of the magnetic field normal to SQUIDs across a single multiplexing column (33 channels) for an axial input field, demonstrating at least a factor of 5000 suppression across the chip. A version of the SQUID enclosure without the high-$\mu$ connector covers shows a factor of 10 worse suppression.

One large high-$\mu$ box, shown in Fig. 3, surrounds the 12 first-stage SQUID daughtercards. This box was simulated separately with COMSOL, using the same $\mu_r = 52000$ as in the previous section. The final mesh contained 316k elements. Figure 6 shows the total field magnitude in the SQUID plane for incident magnetic fields along three

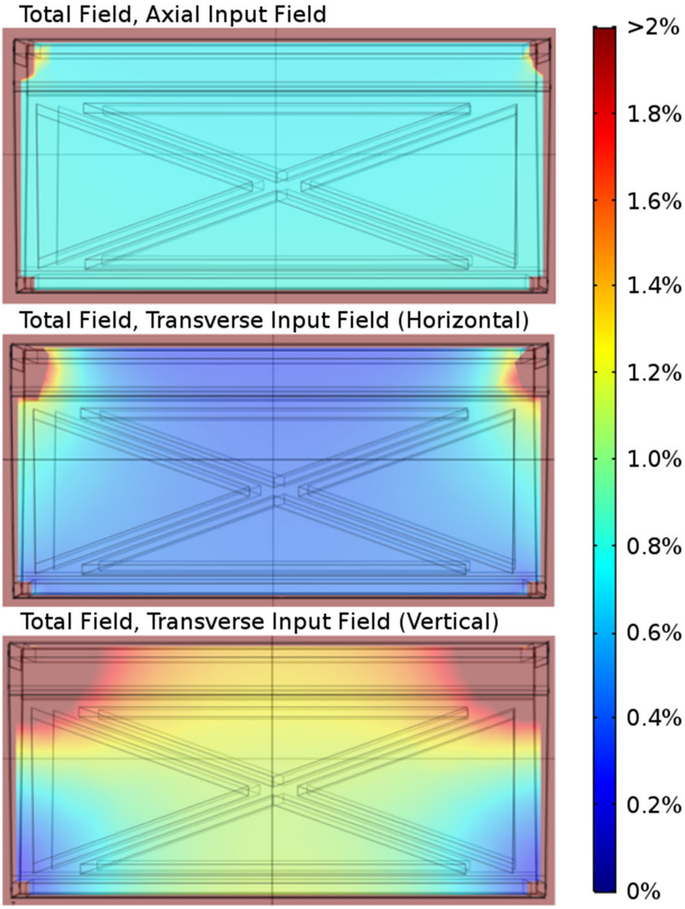


**Fig. 6** COMSOL simulations of the magnetic field suppression of the first-stage SQUID module overshield (high-$\mu$ box). The total magnitude of the magnetic field in the plane of the SQUIDs of the center daughtercard is shown (Color figure online)

axes. The axial field suppression factor is predicted to be $>100$, and the total field suppression factor is predicted to be $>70$ near the SQUIDs.

### 3.2 Cryostat Overshield

A 150-cm-tall high-$\mu$ open-ended cylindrical shield with 1.57-mm-thick walls and a radius of 69 cm sits within the TIME vacuum shield at 300 K. The first-stage SQUID modules sit near the center of this shield (67 cm from the top and 13 cm away from the shield axis) and are shielded further by the high-$\mu$ and superconducting enclosures described in the previous section. The second-stage SQUIDs (at the 4K stage) are located closer to the end of the shield (26 cm from the top and 10 cm from the shield axis) and are enclosed in small Nb boxes that are wrapped in high-$\mu$ material.

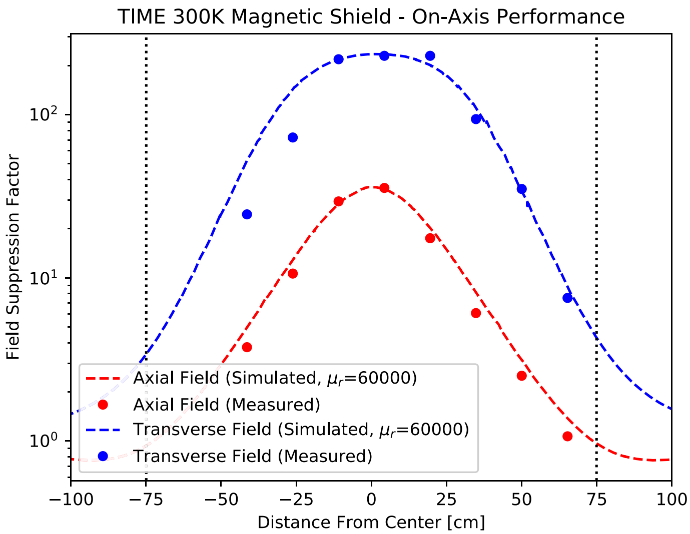


**Fig. 7** Measurements of the TIME high-$\mu$ overshield compared to COMSOL simulations with $\mu_r = 60000$ (Color figure online)

The cylindrical shield was fabricated using Amuneal Amumetal, and the suppression of Earth's magnetic field was measured with a Mag-03MC1000 three-axis magnetic field sensor. Results are plotted in Fig. 7 and are compared to COMSOL simulations using $\mu_r = 60000$ (the value Amuneal advertises [11] at 300 K in 0.5 $\mu$T magnetic fields). The SQUID normal axes (for both stages) are orthogonal to the shield axis, so fields transverse to the cylindrical shield are the most relevant; the suppression factor near the first-stage SQUIDS is approximately 100.

## 4 Conclusions

Hafnium shows promise as a low-$T_c$ alternative to Ti for TIME TESs. Fabrication and testing of TIME detectors with Hf TESs is ongoing.

Magnetic shielding for the TIME first-stage SQUIDs has been presented and simulated, with a predicted total axial field suppression factor of at least $5 \times 10^7$. For comparison, the achieved magnetic field suppression factor for BICEP2 is quoted [10] at $\sim 10^6$.

**Acknowledgements** JH is supported by the National Science Foundation Graduate Research Fellowship under Grant No. DGE-1144469. AC is supported by the National Science Foundation Astronomy and Astrophysics Postdoctoral Fellowship under Grant No. 1602677.

## References

1. J. Hunacek, J. Bock, C.M. Bradford et al., Proc. SPIE **9914**, 99140L (2016)
2. A.T. Crites, J.J. Bock, C.M. Bradford, T.C. Chang, A.R. Cooray, L. Duband, Y. Gong, S. Hailey-Dunsheath, J. Hunacek, P.M. Koch, C.T. Li, R.C. O'Brient, T. Prouve, E. Shirokoff, M.B. Silva, Z.

Staniszewski, B. Uzgil, M. Zemcov, The time-pilot intensity mapping experiment, in [millimeter, submillimeter, and far-infrared detectors and instrumentation for astronomy VII]. Proc. SPIE **9153**, 91531W (2014)

3. J. Hunacek, J. Bock, C.M. Bradford, B. Bumble, T.-C. Chang, Y.-T. Cheng, A. Cooray, A. Crites, S. Hailey-Dunsheath, Y. Gong, M. Kenyon, P. Koch, C.-T. Li, R. O'Brient, E. Shirokoff, C. Shiu, Z. Staniszewski, B. Uzgil, M. Zemcov, Design and fabrication of tes detector modules for the time-pilot [cii] intensity mapping experiment. J. Low Temp. Phys. **184**(3), 733–738 (2016)
4. C.-T. Li, T. Wei, J.-C. Cheng, C. Shiu, A.I. Crites, C.M. Bradford, Development of a millimeter wave grating spectrometer for TIME Pilot, in *The 27th International Symposium on Space Terahertz Technology* (2016)
5. Y. Gong, A. Cooray, M. Silva, M.G. Santos, J. Bock, C.M. Bradford, M. Zemcov, Intensity mapping of the [CII] fine structure line during the epoch of reionization. Astrophys. J. **745**, 49 (2012)
6. M. Silva, M.G. Santos, A. Cooray, Y. Gong, Prospects for detecting CII emission during the epoch of reionization. Astrophys. J. **806**, 209 (2015)
7. C.M. Bradford, B.J. Naylor, J. Zmuidzinas, J.J. Bock, J. Gromke, H. Nguyen, M. Dragovan, M. Yun, L. Earle, J. Glenn, H. Matsuhara, P.A.R. Ade, L. Duband, WaFIRS: a waveguide far-IR spectrometer: enabling spectroscopy of high-z galaxies in the far-IR and submillimeter, in [IR Space Telescopes and Instruments], Mather, J. C., ed. Proc. SPIE **4850**, 1137–1148 (2003)
8. C.M. Bradford, J.E. Aguirre, R. Aikin, J.J. Bock, L. Earle, J. Glenn, H. Inami, P.R. Maloney, H. Matsuhara, B.J. Naylor, H.T. Nguyen, J. Zmuidzinas, The warm molecular gas around the cloverleaf quasar. Astrophys. J. **705**, 112–122 (2009)
9. S. Sah, G. Myneni, & J. Atulasimha (2015). arXiv:1501.07312
10. BICEP2 Collaboration, P.A.R. Ade, R.W. Aikin et al., Astrophys. J. **792**, 62 (2014)
11. http://www.amuneal.com/magnetic-shielding/magnetic-shielding-materials. Retrieved 10 Oct 2017